# Journal of **Prosthodontic Research**

A1 — Disc, F, C, SC

A2 — Anterior, Lateral, Medial, Posterior

## Issue Highlights

- ❖ Effect of partial ferrule on fracture resistance of endodontically treated teeth
- ❖ Radiographic predictive factors for 10-year survival of removable partial denture abutment teeth
- ❖ Current surface modification strategies of polyetheretherketone (PEEK) with bone and soft tissue

## JPR osthodontic esearch

OPEN ACCESS

JPRosthodontic Research

# Journal of Prosthodontic Research

Review article

# Facial scanning technologies in the era of digital workflow: A systematic review and network meta-analysis

Donato Antonacci[a], Vito Carlo Alberto Caponio[b], Giuseppe Troiano[b], Mario Giulio Pompeo[c] Francesco Gianfreda[d], Luigi Canullo[e,*]

[a] Private Practice, Via Leonida Laforgia, 4, 70126 Bari, Italy
[b] Department of Clinical and Experimental Medicine, University of Foggia, Foggia, Italy
[c] Private Practice, Rome, Italy
[d] Department of Industrial Engineering, University of Rome "Tor Vergata", Rome, Italy
[e] Department of Periodontology, University of Bern, Switzerland

## Abstract

**Purpose:** The aim of this network meta-analysis is to evaluate the accuracy of various face-scanning technologies in the market, with respect to the different dimensions of space (x, y, and z axes). Furthermore, attention will be paid to the type of technologies currently used and to the best practices for high-quality scan acquisition.
**Material and Methods:** The review was conducted following the PRISMA guidelines and its updates. A thorough search was performed using the digital databases MEDLINE, PubMed, EMBASE, and the Cochrane Central Register of Controlled Trials by entering research lines or various combinations of free words. The main keywords used during the search process were "photogrammetry", "laser scanner", "optical scanner", "3D, and "face".
**Results:** None of the included technologies significantly deviated from direct anthropometry. The obtained mean differences in the distances between the considered landmarks range from 1.10 to -1.74 mm.
**Conclusion:** Limiting the movements of the patient and scanner allows for more accurate facial scans with all the technologies involved. Active technologies such as laser scanners (LS), structured light (SL), and infrared structured light (ISL) have accuracy comparable to that of static stereophotogrammetry while being more cost-effective and less time-consuming.

**Keywords:** Face-scan, Digital-workflow, Digital dentistry, Virtual patient, Scanning technologies

## 1. INTRODUCTION

The shape and size of the teeth cannot be considered standard characteristics for successful prosthetic treatment. Although these characteristics have average values, they should be adapted individually to the patient's face[1]. In the last few decades, facial scanners have been introduced in orthopedics and plastic surgery for the planning and pre-visualization of the most complex clinical situation[2]. With the introduction of digital workflows in dentistry, photographic protocols have been proposed to obtain an aesthetic preview of smiles[3]. Using computer-aided design (CAD) software, it was possible to contextualize a digital smile wax-up in photographs of the patient in resting or smiling position[4]. However, the images only allow a two-dimensional assessment of the facial planes (orizontal and vertical) and lead to inaccuracies in coupling with the stereo lithography interface (STL) files of the digital wax-up. Facial scans have been proposed in dentistry to overcome this issue. The advantages of these techniques include the possibility of obtaining a

scan of the patient's face in order to contextualize teeth on the facial planes, following the proportions of three-thirds of the face in the most extensive rehabilitation[5], and enabling the identification of the Camper's plane through cutaneous landmarks. Reports on the use of these methods have increased recently in the scientific literature[6]. There are several technologies for acquiring a face scan, such as cone-beam computed tomography (CBCT), which consists of a radiological investigation that is properly used for the diagnosis of hard tissues of the oral cavity, but with a high field-of-view and appropriate segmentation, can "be transformed" in a facial scan[7]. However, limitations in the applicability of this technology include unnecessary radiation exposure. Moreover, different CBCTs are necessary to acquire the patient's face while resting, smiling, and with the mock-up, thereby increasing the general radiation exposure and overall cost. This makes facial scanning using X-ray emission technologies inapplicable in common clinical cases[8]. To achieve better aesthetics and function, prosthetic rehabilitation should be guided by the facial references. 3D digital scans have been used to improve information acquisition procedures and obtain a "so-called" virtual patient[9]. The creation of a "virtual patient" is a modern topic of considerable interest and continuous evolution. This increases the degree of communication with the patient and enhances the various aspects of the daily digital workflow, allowing a better level of plan-

ning in prosthetic, implant, and orthodontic cases [10].

Currently, the most common face scanners in the market use 3D photogrammetry systems, structured light, and laser scanners[11]. Interestingly, there are important differences between these technologies in terms of size and cost. Indeed, the first available scanners in the market had large volumes and were expensive. In recent years, smartphones and tablets with internal cameras capable of capturing surfaces through structured infrared light have been introduced into the market at a cheap price[12]. An important characteristic of these devices is their accuracy, and what has emerged from previous reviews is that this parameter may vary depending on the technology used[6,13]. Many studies aimed at evaluating the accuracy of acquisition systems have considered the linear distance between various facial landmarks[6], while others have considered the difference between surfaces[11]. However, negligible attention has been paid to the spatial distribution of various points on the face[6].

Different points could be used as marks, and while horizontal linear measurements on the X-axis are more suitable for expressive micromovements, the farthest and deepest points (i.e., Tragus) compared to the most prominent points (i.e., Pronasion) may go "out of focus" during the acquisition phase. This could result in a Z-axis acquisition error[13].

The following meta-analysis aims to evaluate the accuracy of the various technologies in the market with respect to the different dimensions of space (x, y, and z axes).

Furthermore, attention will be paid to the type of technologies currently used in dentistry and to the best practices for high-quality scan acquisition.

## 2. MATERIALS AND METHODS

All the different processes required to perform this review follow the guidelines stated in PRISMA and its updates. The protocol was registered in the PROSPERO register (CRD42021275704).

The formulation of the main questions and selection process were performed following the PICO format, as listed below:

**Patients (P):** Healthy patients without transient or permanent facial deformities

**Intervention (I):** Measurement of distance between cephalometric points (En-En, Ex-Ex, Al-Al, Ch-Ch, N-Sn, T-Pg) in three-dimensional facial scans using different scanning technologies, such as static or portable stereophotogrammetry (s-SP or p-SP), structured light (SL), laser scanner (LS), infrared structured light (ISL), and LED structured light (LSL).

**Comparison (C):** same measurements made using direct anthropometry (DA) or other 3D scanning technologies mentioned above.

**Outcome (O):** Accuracy (mm) was estimated by considering the mean difference between the linear measurement of the test technology used and that of direct anthropometry.

### 2.1 Focused questions

Our intent in compiling this review can be summarized by these focused questions:

Which instrument has the lowest accuracy compared to direct anthropometry?

Which of the measurements investigated is most affected by the technology used?

What protocol allows us to obtain clinically accurate scans in daily clinical practice?

### 2.2 Eligibility criteria

All English studies published in the last 22 years, excluding gray literature, case reports, or congress abstracts, investigating the comparisons between different facial scanning technologies on a living patient were included in the systematic review. The following criteria had to be met for inclusion in the network meta-analysis (NMA).

- A minimum of 4 patients in each group reported individual measurements per group with standard deviation (SD).

- Studies or groups that reported the mean values of the selected measures (En-En, Ex-Ex, Al-Al, Ch-Ch, N-Sn, T-Pg) with SD.

### 2.3 Search strategy

A suitable search line was created to run the research in the main digital databases (MEDLINE, PubMed, EMBASE, Cochrane Central Register of Controlled Trials). The following lines have been inserted and adapted to the listed databases: (Mouth, Edentulous/diagnostic imaging OR Dental Impression Technique OR Computer-Aided Design) OR (photogrammetry OR stereo photo OR laser scanner OR optical scanner) AND (face OR facial OR head) AND (3D OR three-dimensional OR three-dimensional) AND (validation OR accuracy OR repeatability OR agreement OR concordance OR reproducibility OR reliability OR reliability OR comparison).

The research was implemented using a free search by entering different combinations of words referring to the searched object. Backward citation search was conducted on the reference list of all identified clinical studies and relevant systematic reviews.

The last electronic search was performed on January 7, 2021. A manual search was also performed in the following journals: British Dental Journal, Journal of Prosthodontic Research, British Journal of Oral and Maxillofacial Surgery, Clinical Implant Dentistry and Related Research, Clinical Oral Implants Research, Clinical Oral Investigations, European Journal of Oral Sciences, Implant Dentistry, International Journal of Oral and Maxillofacial Implants, International Journal of Periodontics and Restorative Dentistry, Journal of Dental Research, Journal of Dentistry, Journal of Maxillofacial and Oral Surgery, and Journal of Oral and Maxillofacial Surgery.

### 2.4 Study selection

The selection process was independently completed by two authors (DA and FG). Articles were initially selected based on their title and abstract, and then the full texts of the most relevant articles were

reviewed. Once the full text was screened, the articles were either included in the quantitative analysis or only in the qualitative analysis. If differing positions or concerns were found among authors, they were resolved in consultation with a third author (LC). Interrater reliability (IRR) was assessed to estimate the concordance of the authors in the selection process and exclusion criteria codes. IRR was measured through Cohen's k coefficient and the result was interpreted as ≤0 (indicating no agreement), 0.01–0.20 (none to slight), 0.21–0.40 (fair), 0.41– 0.60 (moderate), 0.61–0.80 (substantial), and 0.81–1.00 (almost perfect agreement). A score of ≥80% was considered adequate to satisfy the IRR.

## 2.5 Data collection

Data were extracted and collected from two worksheets. The first worksheet included the characteristics of all studies, such as technology used, space planes investigated, number of landmarks used, measurement technique (linear or surface), complications reported, image acquisition time, price, and study results. The price was judged to be below 500, affordable between 500 and 5000, and expensive above 5000 euros. Eight cephalometric points were considered for data collection, the choice was made by looking at the most common points in papal studies: Endocantion (En) medial corner of the eye, Exocantion (Ex) lateral corner of the eye, Alare (al) wing of the nose, Chelion (Ch) corner of the mouth where the upper and lower lips join, Nasion (n) unequal and median point located at the root of the nose, Subnasal (Sn) midpoint located between the base of the columella and the upper lip, Tragus (t) triangular protrusion near auricle, Pogonion (Pg) the most anterior point of the "tip" of the jaw. The second table presents the data inherent in the quantitative analysis with respect to En-En, Ex-Ex, Al-Al, Ch-Ch, n-Sn, and t-Pg.

## 2.6 Risk of bias assessment

The QUADAS-2 tool was used to assess the quality of the studies included in the NMA [14]. Two authors (DA and VCAC) separately screened the domains of the QUADAS-2 instrument by assigning a score for risk of bias and another for application concern. A third author (LC) was involved in cases with questionable or controversial ratings. The domains of the risk of bias were patient selection (domain 1), index test (domain 2), reference standards (domain 3), and flow and timing (domain 4). Each domain can be judged as low risk, high risk, or unclear. If two domains were considered unclear, the study was considered to have a possible inclusion of bias, whereas if more than two domains were considered unclear or one was considered high risk, the study was at high risk of bias. In the application concern, the same domains listed above are present, except for the flow and timing. In this case, even if only one domain was considered unclear, the study had the potential risk of including applicability concerns; if more than one domain was considered negative, the study had strong applicability concerns. To graphically visualize the reliability of the comparisons made through data analysis, the edges connecting the groups in the network plot were colored as follows: green (high reliability), yellow (moderate reliability), and red (low reliability).

## 2.7 Data analysis

The extracted data were pooled to fit the STATA software network setup command. Data were grouped based on the standard device versus the experimental one, according to the different measured points (en-en, ex-ex, al-al, ch-ch, n-sn, t-pg). Relevant assumptions such as similarity, transitivity, and consistency were assessed. Similarity was qualitatively assessed in the included studies by evaluating the population, intervention, comparison, and outcome. Transitivity was further assessed by statistically investigating the consistency between the outcomes of the direct and indirect comparisons. Once these assumptions were tested, a network map was generated. Different node sizes and line thicknesses allowed us to present information based on study weight, such as the number of studies presenting those comparisons and the number of patients included. A contribution plot was generated to quantitatively inspect the role of each study in direct and indirect comparisons and in the entire network setup. Network meta-analysis means that summary effects together with their predictive intervals are presented to facilitate the interpretation of results. The forest plot of the estimated summary effects, incorporating confidence intervals and predictive intervals, displays the relative mean effects and predictions for each comparison. NMA was performed using mvmeta network commands in the STATA software suggested by Chaimani et al[15–17].

To investigate the sagittal plane, in two studies[18,19], the tragus-menton (T-Me) measurement, as well as the tragus-gnation (t-gn), were considered to be merged with the tragus-pogonion (t-Pg) measurement. These distances were mainly located in the sagittal plane, with small differences in length and position, which did not affect the mean difference.

# 3. Result

The identification of studies through databases resulted in 2684 articles excluding duplicates. After title and abstract screening, the full texts of 70 articles were retrieved and assessed. Of these, 19 were excluded for not investigating accuracy, 10 for not investigating living subjects, and 12 for not considering linear measurements or surface-to-surface deviations. At the end of the selection process 29[9,18–45] articles were included in the systematic review and qualitative analyses. The IRR score from Cohen's k statistic was 0.84 (84%), suggesting substantial agreement between the reviewers at the full-text article selection stage. Further details of the selection process are presented in the flowchart (**Fig. 1**). The studies were distributed over the period from 2004 to 2021, involving a total of 668 patients (**Table 1**). The vertical (Y) and horizontal (X) planes were investigated in all articles, whereas 17 studies reported information on the sagittal plane (Z).

## 3.1 Qualitative synthesis

Among the 29 studies included in the systematic review, different study groups were identified: the most common control group was direct anthropometry. Among the studied groups, static-stereophotogrammetry was the most represented with 14 study groups[9,10,19,23-26,29,31,36,38,43]; eight studies investigated infrared structured light[9,12,35,38,39,42-45]; six studies considered portable-stereophotogrammetry[32-34,39-41] and structured light[9,20,28,30,37,38], while laser scanners[18,21,22,27,40] were investigated in five groups. Only one study reported the use of LED structured light[9].

The measurement technique and number and type of landmarks used for the assessment were collected. Seventeen studies[12,18-20,22-28,31,32,36-39] investigated only linear measures using a range of 6–48 landmarks, four studies[21,40,43,44] investigated both linear and angular measures, and four[34,42,45] investi-
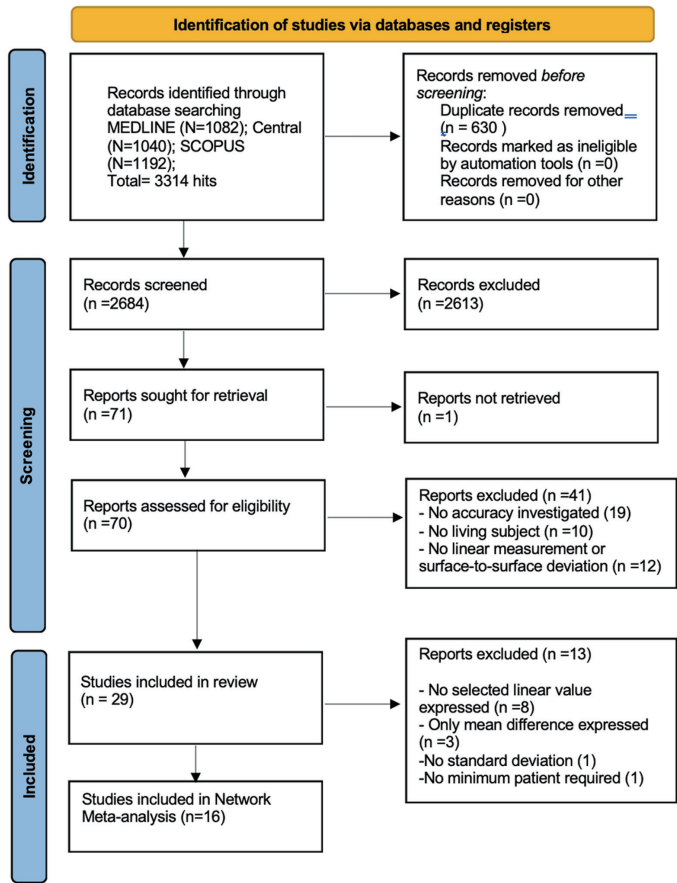
**Fig. 1.** Flowchart of the study selection process

gated both linear measures and surface-to-surface deviation. Three types of measurements were employed in two articles[29,33], and two[9,30] additionally investigated surface-to-surface deviation only.

The longest scanning time was attributed to the use of laser scanner with about 30 s[18,21]. On the contrary the fastest were the static-stereophotogrammetry technologies between 0.03 and 0.09 s [9,19,20,23-26,28-30,33-36,38,41,43]. Structured light requires 20 s and 10 s[28,30,37,38], portable-stereophotogrammetry[32-34,39-42], and new laser scanners[22,27,40]. In the case of infrared structured light, scanning times varied between 5 and 30s[9,12,30,35,38,39,42-45] because they were influenced by the presence of a single unit or several units, which considerably reduced the time. It also depends on the software used for scanning and the type of device that supports the application.

Static-stereophotogrammetry and laser scanners were the most expensive technologies and were also the most investigated in 22 studies. SL and p-SP fall into the affordable category, and ISL, used in the most recently published articles, were the cheaper technologies. However, when ISL technology is used by the implementation of multiple units, the cost increases slightly and the technology falls into the affordable category[44].

### 3.2 Quality Assessment and Applicability Concern (Fig. 2)

The QUADAS-2 tool was used to investigate the risk of incor-

porating errors into the study protocol, outcomes, and applicability. Among the 16 studies included in the NMA, only 4[19,22,25,43] were considered to have a moderate level of introducing errors. Domain 2 is often referred to as "Unclear" because, in some studies[18,19,22,26,27,31,43,45], no information about assessor blindness has been reported. In other studies, the Domain 3 was considered "Unclear" because the DA measures, considered the gold standard technique, were not reported[28,33,43] and these were essential to have a reference to compare the data of the test group. Four studies[19,22,26,44] were judged "Unclear" on Domain 4 because the possibility of unusable facial scans was not resolved clearly. Some concerns regarding applicability were met in one study[27] regarding the patient selection domain. Patients in this study were recruited from the staff of the orthodontic clinic and, therefore, may have had long-standing training on the issue. Studies that had strict inclusion criteria, such as patients with no beard, no moustache, short hair, or hair tied to overcome possible errors introduced by these facial parts, were not considered limitations to applicability because in order to identify points such as the subnasal, tragus, and nasion, it is necessary to have these areas free from facial hair.

### 3.3 Network Meta-Analysis

Sixteen articles[18-20,22,25-28,31,33,35,36,42-45] were analyzed quantitatively. The studies recruited more women than men, with ages ranging from 16 to 74 years old.

In the included articles, all the above-mentioned technologies were used; the most represented was s-SP in nine study groups[19,25,26,28,31,33,35,36,43], whereas p-SP was only reported by one author[31]. ISL technology was adopted in five studies[35,42-45] and was the second most reported device in the NMA, followed by SL[20,28] and LS[18,22,27].

#### 3.3.1 En-En

Eleven studies were included in the NMA[19,20,25-28,31,35,42-44]. The generated network geometry plot is shown in **Figure 3A**. The s-SP-DA comparison was one of the most common comparisons included in this NMA and had a medium risk of bias. The contribution plot (**Fig. 3B**) shows that DA-LS was entirely made of direct comparison and it alone was the second most influential for the whole network (23.5%). DA-ISL was made almost entirely by direct comparisons (95.2%) and resulted in the highest influence in the entire network (23.6%) and contributed 48.2% in the indirect comparison of ISL-LS, with DA-LS, which indirectly contributed 49.4%. Inconsistency was not found at the global level (p =0.88), which was confirmed by the local inconsistency test (DA-ISL p-value=0.65, DA-SL p-value=0.66, DA-s-SP p-value=0.90, ISL-s-SP p-value=0.65, and SL-s-SP p-value=0.66). Inconsistency was visually checked in the network forest plot, which confirmed the absence of inconsistency by graphically representing the effect sizes by study (**Fig. 3C**). The effect size of the device is shown in the interval plot (**Fig. 3D**). All devices, such as ISL, LS, SL, and s-SP, were close to the null-effect line, showing comparable results to DA. However, they exhibited high C.Is. and P.Is., which could be used in future studies to produce over or underestimated measurements.

#### 3.3.2 Ex-Ex

Thirteen studies dealing with ex-ex measurements were included in the NMA[18-20,25,27,28,31,35,42-45]. The study by Gibelli et

**Table 1.** Characteristics of studies. This table report the relevant characteristics of the studies considered in the systematic review.

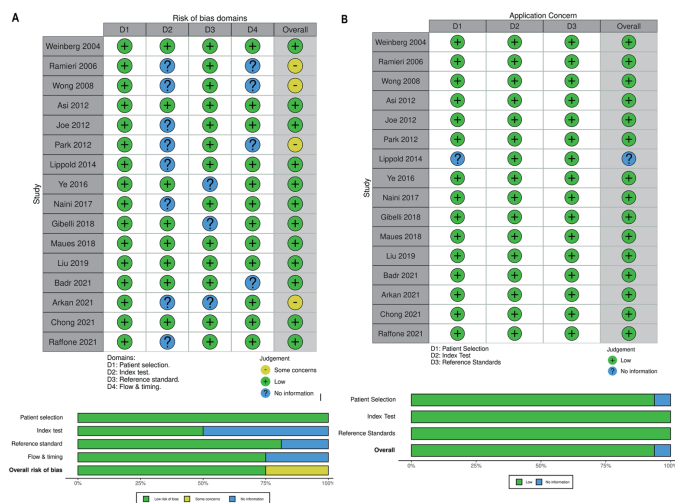| Author/Year | Subject | Test | Test Code | Control | Control Code | Spatial Plane | No. Landmark and placement time | Measuring Technique | Scanning Time | Price | Outcome |
|---|---|---|---|---|---|---|---|---|---|---|---|
| **Weinberg 2004** | 20 | Structured light | SL | Direct Anthropometry | DA | Horizontal, Vertical, Sagittal | 17, pre-scanning | 19 Linear distances | 0,5s (Genex tech-Rainbow 3D) | Affordable | Results indicate very high levels of precision (particularly when facial landmarks were labeled) and fairly good congruence with traditional (1-3 mm) |
| **Kovacs 2006** | 5 | Laser scanner | LS | Direct Anthropometry | DA | Horizontal, Vertical, Sagittal | 48, pre and post scanning | 680 linear distances and angles | 30 s (Minolta-vivid910) | Expensive | The best accuracy is obtained with the head at +10°, illuminated place and with more cameras while keeping the patient still. |
| **Ramieri 2006** | 5 | Laser scanner | LS | Direct Anthropometry | DA | Horizontal, Sagittal | 12, pre-scanning | 6 linear distances | 17 s (Head and Face Colour 3D Scanner Cyberware) | Expensive | The development of a specific protocol resulted in a mean scanning error of 1–1.2 mm. |
| **Ghoddusi 2007** | 6 | Static-Stereophotogrammetry | s-SP | Direct Anthropometry | DA | Horizontal, Vertical, Sagittal | 14, pre-scanning | 15 linear distances | 0,09 s (Surface Imaging International Ltd.) | Expensive | Measurements recorded by the 3D system appear to be both sufficiently accurate. (1-3 mm) and reliable enough for clinical use. |
| **Wong 2008** | 20 | Static-Stereophotogrammetry | s-SP | Direct Anthropometry | DA | Horizontal, Vertical | 19, post-scanning | 18 linear distances | 0,09 s (3dMD face system) | Expensive | 3dMDface System is valid and reliable. Digital measurements may require direct marking, prior to imaging. |
| **Heike 2009** | 20 | Static-Stereophotogrammetry | s-SP | Direct Anthropometry | DA | Horizontal, Vertical, Sagittal | 26, pre-scanning | 30 linear distances | 0,09 s (3dMD face system) | Expensive | The Pearson correlation coefficients of greater than 0.9 for most distances. Three-dimensional image-based measurements were larger for the head length and width, forehead widths, and upper and lower facial widths. |
| **Asi 2012** | 20 | Static-stereophotogrammetry | s-SP | Direct Anthropometry | DA | Horizontal, Vertical | 17, pre-scanning | 18 linear distances | 0,035 s (VectraXT) | Expensive | Only 5/11 measurements have significant difference however are not clinically significant difference because the mean errors are less than one millimetre. |
| **Joe 2012** | 9 | Laser scanner | LS | Direct Anthropometry | DA | Horizontal, Vertical, Sagittal | 14, pre-scanning | 10 linear distances | 30 s (Minolta-vivid9i) | Expensive | Seven of the ten measurements collected were found to be accurate, with mean differences falling within the acceptable margin of error (1–3 mm). |
| **Park 2012** | 20 | Static-Stereophotogrammetry | s-SP | Direct Anthropometry | DA | Horizontal, Vertical | 7, pre-scanning | 5 linear distances | 0,03 s (Di3D camera system) | Expensive | The magnitude of differences was very small (mean = 0.73 mm). Good congruence was observed between the means derived from the Di3D system and the digital calliper. |
| **Lippold 2014** | 15 | Laser scanner | LS | Direct Anthropometry | DA | Horizontal, Vertical | 12, post-scanning | 7 linear distances | 15 s (FastSCAN- Polhemus) | Affordable | Most of the errors or differences to manual measurements were below 1mm and only a few extended to 2 mm. |
| **Ye 2016** | 10 | Structured light | SL | Static-Stereophotogrammetry | s-SP | Horizontal, Vertical | 16, pre-scanning | 21 linear distances | T: 12 s (3D CaMega-BWHX) C: 0,09 s (3dMD face) | T: Expensive C: Expensive | Lin's CCC showed substantial agreement between digital and manual measurements for 4 of the 7 distances evaluated. Larger discrepancies were due to inadequate image quality and scanning errors. |
| **Dindaroglu 2016** | 80 | Static-Stereophotogrammetry | s-SP | Direct Anthropometry | DA | Horizontal, Vertical, Sagittal | 17, pre-scanning; 3D point clouds | 10 linear distances/ 6 angles/ surface deviation | 0,09 s (3dMD face system) | Expensive | The difference was less than 2 mm for all parameters. |
| **Modabber 2016** | 41 | Structured light | SL | Portable-Structured light | p-SL | Horizontal, Vertical, Sagittal | 2 Lego brick | Surface deviation | T: 15 s (FaceScan3D) C: 20s (Artec 3D eva) | T: Affordable C: Expensive | Scanning with Artec EVA leads to more accurate 3D models as compared to scanning with FaceScan3D |
| **Naini 2017** | 6 | Static-Stereophotogrammetry | s-SP | Direct Antropometry | DA | Horizontal, Vertical, Sagittal | 14, post-scanning | 15 linear distances | 0,09 s (3dMD face system) | Expensive | The overall median percentage difference was just 4%, highlighting good agreement between the two methods. |
| **Knoop 2017** | 8 | T1: Infrared Structured light T2: LED Structured light | ISL/ LSL | C: Static-Stereophotogrammetry | s-SP | Horizontal, Vertical, Sagittal | 3D point clouds | Surface deviation | T1: 20 s (iPad 4th generation) T2: 30 s (M4D Scan) C: 0,015 s (3dMD face system) | T1: Economic T2: Expensive C: Expensive | The M4D Scan showed significantly best RMS, better than the Avanto MRI and Structure Sensor. |

**Table 1.** Continued.

| Author/Year | Subject | Test | Test Code | Control | Control Code | Spatial Plane | No. Landmark and placement time | Measuring Technique | Scanning Time | Price | Outcome |
|---|---|---|---|---|---|---|---|---|---|---|---|
| **Kim 2018** | 5 | T1: Portable stereophotogr. T2: static-stereophotogrammetry | p-SP/s-SP | Direct Anthropometry | DA | Horizontal, Vertical, Sagittal | 29, pre-scanning | 25 linear distances | T1=10 s (vectraV1-Canfield) T2: 0,035 s (Vectra M3) | T1: Affordable T2: Expensive | Bias measurements revealed that the handheld and conventional camera methods yielded larger measurements than direct callipers |
| **Gibelli 2018** | 51 | Portable-stereophotogrammetry | p-SP | Static-Stereophotogrammetry | s-SP | Horizontal, Vertical | 17, pre-scanning; 3D point clouds | 14 linear distances/12 angles/volumes/surfaces | T: 10 s (vectraV1-Canfield) C: 0,035 s (Vectra M3) | T: Affordable C: Expensive | High reliable for assessing linear, measurement, angle and surface. Less reliable for volume and RMS distance. |
| **Camison 2018** | 27 | Portable-Stereophotogrammetry | p-SP | Static-Stereophotogrammetry | s-SP | Horizontal, Vertical, Sagittal | 17, pre-scanning; 3D point clouds | 136 linear distances/Surface deviation | T:10 s (vectraV1-Canfield) C: 0,09 s (3dMD face system) | T: Affordable C: Expensive | Areas exceeding ±1 mm were limited to facial regions containing hair or subject to facial microexpressions. |
| **Maues 2018** | 10 | Static-Stereophotogrammetry | s-SP | Infrared Structured light | ISL | Horizontal, Vertical, Sagittal | 10, 3D point clouds | 7 linear distances, Surface deviation | T: 0,03 s (Di3D camera system) C: 30 s (Kinect-Microsoft) | T: Expensive C: Economic | Using Kinect the model quality depends greatly on the patient's ability to stay still during the process. Scanning with Di3D leads to more accurate 3D models as compared to scanning with Kinect. |
| **Liu 2019** | 12 | Static-Stereophotogrammetry | s-SP | Direct Anthropometry | DA | Horizontal, Vertical | 8, pre-scanning | 8 linear distances | 0,1 s (Canon EOS 1200D; Canon Europe) | Affordable | The mean ±standard deviation difference between the clinical and digital measurements was 1.95 ± 0.33 mm. |
| **de Sa Gomes 2019** | 15 | Structured light | SL | Direct Anthropometry | DA | Horizontal, Vertical, Sagittal | 12, pre-scanning | 11 linear distances | 14 s (Artec 3D eva) | Expensive | Marking of points on the face before the scan there is a reduction in the time needed to accomplish the measures. |
| **Koban 2019** | 15 | Infrared structured light/ Structured light | ISL/SL | Static-photogrammetry | s-SP | Horizontal, Vertical | 3D point clouds | 7 linear distances | T1: 12,1 s (Sense 3D) T2: 14 s (Artec 3D eva) C: 0,035 s (VectraXT) | T1: Economic T2: Expensive C: Expensive | Sense 3D showed promising results, but could not accurately capture more complex surfaces, including the nasal and facial margins. |
| **Rudy 2020** | 16 | Infrared structured light | ISL | portable-Stereophotogrammetry | p-SP | Horizontal, Vertical | 10, post-scanning | 9 linear distances | T: 20 s (iPhone X, ScandyPro App, New Orleans) C: 10 s (vectraH1-Canfield) | T: Economic C: Affordable | The mean absolute measurement error between landmark-to-landmark surface distances on Vectra H1–derived models and the same distances performed on iPhone X–derived models was 0.46 ± 0.01 mm. |
| **Ayaz 2020** | 50 | Laser scanner/ Portable-Stereophotogrammetry | LS/p-SP | Direct Anthropometry | DA | Horizontal, Vertical | 17, post-scanning | Linear distances and angles | T1:20 s (Proface-Planmeca) T2: C: 10 s (vectraH1-Canfield) | T1: Expensive T2: Affordable | The 2D photographs displayed the highest combined total error for linear measurements. SPG performed better than LS, with borderline significance |
| **Piedra Cascon 2020** | 10 | Infrared structured light | ISL | Direct Anthropometry | DA | Horizontal, Vertical | 6, pre-scanning | 5 linear distances | 10 s (Huawei MediaPad M3, FaceApp-Bellus 3D) | Economic | The dual-structured light facial scanner obtained a trueness mean value of 0.91 mm and a precision mean value of 0.32 mm. |
| **White 2020** | 36 | Static-Stereophotogrammetry | s-SP | Portable-Stereophotogrammetry | p-SP | Horizontal, Vertical, Sagittal | 19, post-scannig; 3D point clouds | Surface deviation | T: 0,09 s (3dMD face system) C: 10 s (vectraH1-Canfield) | T: Expensive C: Affordable | Accounting for this technical error, participant movement adds less than ~0.1 mm additional variation, with the total average difference between sequential images of the same person being 0.40 mm (Vectra H1) and 0.44 mm (3dMDface). |
| **Chong 2021** | 20 | Infrared structured light | ISL | Direct Anthropometry | DA | Horizontal, Vertical, Sagittal | 18,post-scanning; 3D point clouds | 21 linear distance and surface deviation | T1: 11 s (MeiXuan- App iOS) T2: 10s (vectraH1-Canfield) | T: Economic | The Mean Absolute Difference were less than 1 mm in 15 of 21 parameters. No parameter had a MAD over 1.50 mm. |
| **Akan 2021** | 26 | Infrared structured light | ISL | Static-Stereophogrammetry | s-SP | Horizontal, Vertical | 9, pre-scanning | 7 linear distance and 2 angular | T: 10 s (Iphone X-FaceApp-Bellus 3D) C: 0,09 s (3dMD Face camera) | T: Economic C: Affordable | Statistically significant changes were found in distance between inner commissures of right and left eye fissure and nasolabial angle. |

**Table 1.** Continued.

| Author/ Year | Sub-ject | Test | Test Code | Control | Con-trol Code | Spatial Plane | No. Land-mark and placement time | Measuring Technique | Scanning Time | Price | Outcome |
|---|---|---|---|---|---|---|---|---|---|---|---|
| **Badr 2021** | 80 | Infrared structured light (multiple units) | ISL | Direct Anthro-pometry | DA | Horizontal, Vertical, | 10, pre-scanning | 10 linear distance and 6 angular | < 5s (Kinect-Micro-soft) | Affordable | In this study, the mean difference was found to be 0.5 mm between DA and ISL |
| **Raffone 2021** | 10 | Infrared structured light | ISL | Direct Anthro-pometry | DA | Horizontal, Vertical, Sagittal | 17, pre-scanning; 3D point clouds | 23 linear distance and surface deviation | 10 s (Ipad Pro 3rd,FaceApp-Bellus 3D) | Economic | The use of Slider Tecnique is suggest-ed for a reliable clinical use due to the better precision and an effective reduction of motion artefacts and the lower compliance required to the patients during the scan. |

DA= direct anthropometry, NR=not reported,y= years, mo=months, w=weeks, s-SP= Static Stereophotogrammetry, p-SP= portable Stereophotogramme-try, SL= Structured light, LS=Laser Scanner, ISL=Infrared Structured Light, LSL=LED Structured Light.



**Fig. 2.** QUADAS-2 tool: (A) risk of bias and (B) application concerns

al.[33] was excluded because the results were inconsistent. The gen-erated network geometry plot is shown in **Figure 4A**. Comparison between ISL and s-SP resulted in only one medium risk of bias.

DA-LS comprised almost all direct comparisons (99.8%) and contributed 38.8% in the indirect comparison of ISL-LS with DA-LS, which indirectly contributed 45.5%. DA-ISL and DA-SL made direct comparisons in 71.1% and 71.9% of cases, respectively. DA-ISL was the most significant contributing factor in the entire network (25.7%), followed by DA-LS (22.3%) (**Fig. 4B**).

Although some comparisons showed inconsistency, global in-consistency was assumed to be absent (p =0.065) (**Fig. 4C**). The ef-fect size of the device is shown in the interval plot (**Fig. 4D**).

LS was overestimated in comparison with DA, whereas s-SP re-sulted in underestimation compared to DA. The ISL was the most comparable to DA.

### 3.3.3 Ch-Ch

Thirteen studies dealing with ch-ch measurements were includ-ed in the NMA[18,20,25,27,28,31,33,35,36,42,44,45]. The generated

network geometry plot is shown in **Figure 5A**. Overall, a low risk of bias was assessed for all comparisons. The contribution plot showed that the DA-LS comparison was given only by direct contrast and the same for the p-SP-s-SP comparison. DA-SL was mainly constituted by direct comparison (76.7%) and contributed 42.7% to the indirect comparison of ISL-SL. DA-ISL was the most influential comparison in the entire network (19.7%) against SL-s-SP, contributing only 4.1% (**Fig. 5B**). Inconsistency was not found either at global (p-value=0.98) or local level (DA-ISL p-value=0.95, DA-SL p-value=0.84, DA-s-SP p-value=0.95, ISL-s-SP p-value=0.95, SL-s-SP=0.84 and p-SP-s-SP p-value=0.99).This result was confirmed while evaluating the network forest plot, where it is possible to graphically represent effect size by study (**Fig. 5C**). The effect size of the device is shown in the inter-val plot (**Fig. 5D**). ISL and LS were overestimated in comparison with DA, while p-SP, s-SP, and SL were underestimated compared to DA, although their large C.Is. and P.Is. could result in over-or underesti-mated measurements in future studies.

### 3.3.4 AI-AI

Eleven studies dealing with all measurements were included in the NMA[18-20,22,25,27,35,42,44,45]. The generated network geom-etry plot is presented in **Fig. 6A**, showing an overall low risk of bias in most of the comparisons, but s-SP-DA, for which medium bias was found. DA was the main comparator among all the direct compari-sons. The contribution plot showed that DA-SL and DA-LS compari-sons were given by only direct contrasting, and together contributed equally (50%) to the indirect estimates of LS-SL. The s-SP-ISL com-parison was the least influential contributor in the whole network, accounting for 6.5%, while DA-ISL, DA-LS, and DA-SL contributed equally to the entire network, accounting for 24.2% (**Fig. 6B**). Incon-sistency was not found at either the global or local level (p =0.19). This result was confirmed when evaluating the network forest plot, where it was possible to graphically represent the effect size by study (**Fig. 6C**), and the effect size by device is shown in the interval plot (**Fig. 6D**). ISL and SL were mostly comparable and overestimated in comparison with DA, whereas LS was the most comparable to DA, al-though its large C.Is. and P.Is. could result in over-or underestimated measurements in future studies.

### 3.3.5 N-Sn

Fifteen studies were included in the NMA[18-20,25-28,31,33, 35,42-45]. The generated network geometry plot is shown in **Fig. 7A**, which shows a medium risk of bias in the comparison of s-SP-DA

**Table 2.** Results. This table report the measurement of test and control groups of the NMA included studies.

| Author Year | Gender (M/F) | Age (mean±SD /or range) | Test | N patient Test | Control | N patient Control | Horizontal | | | | | | | | Vertical | | Sagittal | |
|---|---|---|---|---|---|---|---|---|---|---|---|---|---|---|---|---|---|---|
| | | | | | | | En-en | | Ex-Ex | | Al-Al | | Ch-Ch | | N-Sn | | T-Pg | |
| | | | | | | | T | C | T | C | T | C | T | C | T | C | T | C |
| Weinberg (a) 2004 | 6/14 | 16 to 62 y | SL | 20 | DA | 20 | | | 87,06 (4,87) | 87,74 (5,13) | 33,66 (2,44) | 32,85 (2,66) | 50,33 (3,89) | 51,12 (3,92) | 55,58 (3,34) | 56,55 (3,28) | 141,77 (11,20) | 138,36 (7,68) |
| Weinberg (b) 2004 | 6/14 | 16 to 62 y | SL | 20 | DA | 20 | 30,28 (2,57) | 30,75 (2,53) | 89,76 (4,45) | 89,39 (4,07) | 32,86 (2,61) | 32,58 (2,46) | 49,04 (4,08) | 49,56 (3,92) | 54,70 (3,25) | 55,49 (3,36) | 139,5 (7,38) | 142,42 (7,94) |
| Ramieri 2006 | 4/2 | 27.5 y | LS | 6 | DA | 6 | | | | | 35,65 (0,47) | 35,65 (0,41) | | | | | 143,8 (0,60) | 143,75 (1,50) |
| Wong 2008 | 12/8 | 20 to 40 y | s-SP | 20 | DA | 20 | 32,3 (4) | 31,1 (3,9) | 90,4 (5,3) | 91,1 (4,5) | 35,1 (3,8) | 35,6 (4) | | | 52 (3,5) | 51,2 (3) | | |
| Asi 2012 | 10/10 | 20 to 29 y | s-SP | 20 | DA | 20 | 32,8 (3,20) | 32,69 (3,20) | 93,72 (5,04) | 100,09 (5,78) | 37,61 (3,07) | 37,13 (2,96) | 48,78 (3,13) | 48,95 (2,94) | 56,01 (5,83) | 55,65 (55,65) | | |
| Joe 2012 | 4/5 | 22 to 43 y | LS | 9 | DA | 9 | | | 97,6 (5,9) | 93,8 (6,10) | 35,9 (4,90) | 33,3 (5,2) | 52,0 (3,50) | 50 (3,80) | 51,8 (3,40) | 51,10 (51,1) | 307,2 (30,2) | 307,7 (30,3) |
| Park 2012 | 10/10 | 23 to 50 y | s-SP | 20 | DA | 20 | 31,76 (2,17) | 31,38 (3,43) | | | | | | | 67,91 (3,67) | 66,38 (3,64) | | |
| Lippold 2014 | 10/5 | 21 to 40 y | LS | 15 | DA | 15 | 25,90 (2,68) | 25,98 (2,87) | 99,65 (5,46) | 100,37 (6,05) | 33,47 (2,48) | 34,11 (2,61) | 51,12 (3,92) | 51,49 (2,56) | 50,36 (3,78) | 49,30 (3,25) | | |
| Ye 2016 | 5/5 | 23 to 30 y | SL | 10 | s-SP | 10 | 35,81 (2,49) | 35,77 (2,14) | 99,2 (5,43) | 99,30 (5,68) | | | 52,05 (5,17) | 51,43 (5,17) | 55,15 (4,59) | 54,77 (4,59) | | |
| Naini 2017 | 2/4 | NR | s-SP | 6 | DA | 6 | 30,08 (1,73) | 30,87 (1,76) | 89,21 (3,88) | 92,90 (4,06) | | | 49,93 (3,90) | 52,85 (3,70) | 57,53 (4,74) | 60,05 (4,33) | 131,87 (7,27) | 132,70 (8,92) |
| Maues 2018 | 5/5 | NR | s-SP | 10 | ISL | 10 | 31 (2,62) | 33,51 (2,32) | 92,20 (5,46) | 94,01 (5,65) | 34,97 (3,16) | 37,95 (3,63) | 49,00 (2,84) | 50,22 (3,14) | 59,15 (4,26) | 59,39 (4,43) | 144,2 (7,4) | 143,2 (7,5) |
| Gibelli 2018 | 16/34 | 19 to 61 y | p-SP | 50 | s-SP | 50 | | | 88,5 (4,7) | 86,5 (3,0) | | | 50,3 (4,3) | 50,7 (4,1) | 55,80 (3,60) | 55,20 (55,2) | | |
| Liu 2019 | 7/5 | 74.6 years | s-SP | 12 | DA | 12 | | | 119,64 (7.75) | 118.64 (7.30) | | | 59.36 (5.87) | 61,43 (5,59) | | | | |
| Badr 2021 | 48/32 | 25 to 45 y | ISL | 80 | DA | 80 | 29,64 (2,04) | 29,64 (2,04) | 109,90 (3,86) | 109,88 (3,86) | 35,54 (2,32) | 35,54 (2,33) | 49,53 (3,51) | 49,53 (3,51) | 56,91 (7,25) | 56,91 (7,25) | | |
| Arkan 2021 | 16/10 | NR | ISL | 26 | s-SP | 26 | 31.35 (2.34) | 33.34 (2.78) | 94.52 (3.99) | 95.41 (3.79) | | | | | 53.11 (3.43) | 53.77 (3.52) | | |
| Chong 2021 | NR | 18 to 30 y | ISL | 20 | DA | 20 | 35,83 (2,86) | 35,49 (2,74) | 87,01 (3,99) | 86,31 (3,87) | 29.58 (2,82) | 29,59 (2,81) | 44,69 (4,85) | 44,64 (4,71) | 44,08 (4,52) | 43,44 (4,53) | 121,27 (8,52) | 121,21 (9,12) |
| Raffone 2021 | 6/4 | 29 to 62 y | ISL | 10 | DA | 10 | | | 124,84 (0,63) | 122,91 (0,01) | 50,89 (0,58) | 49,63 (0,01) | 79,68 (1,09) | 79,02 (0,01) | 67,84 (0,58) | 68,04 (0,01) | | |

DA= direct anthropometry NR=not reported,y= years, mo=months, w=weeks, s-SP= Static Stereophotogrammetry, p-SP= portable Stereophotogrammetry, SL= Structured light, LS=Laser Scanner, ISL=Infrared Structured Light.

and s-SP-ISL. The contribution plot showed that the DA-ISL, DA-LS, and p-SP-s-SP comparisons were almost completely direct, at 94.8%, 99.9%, and 96.4%, respectively. DA-ISL and DA-LS contributed 48.1% and 49.3%, respectively, to the indirect comparison of ISL-LS. DA-ISL was the main contributing factor to the entire network (21.5%), followed by DA-LS (16.9%) (**Fig. 7B**).

Inconsistency was not found at either the global (p-value=0.63) or local level (DA-ISL p-value=0.77, DA-SL p-value=0.40, DA-s-SP p-value=0.49, ISL-s-SP p-value=0.77, SL-s-SP p-value=0.40, and p-SP-s-SP p-value=1). This result was confirmed by evaluating the network forest plot (**Fig. 7C**).

ISL showed interesting results (**Fig. 7D**), with small C.I. and P.I., comparable to DA. LS and SL were marginally over- and underestimated, respectively, compared with DA, showing small C.Is. and P.Is. p-SP showed very large C.I. and P.I. values, which could be used in future studies to produce over-or underestimated measurements.

*3.3.6 T-Pg*

Linear distance represents the sagittal Z-axis component. NMA included eight studies[18-20,22,31,35,42]. The generated network geometry plot is represented in **Fig. 8A**, showing a medium risk of bias in both the LS and s-SP comparisons against DA. The contribution plot showed that the DA-LS was determined entirely by direct comparison. DA-LS and DA-SL contributed 50% and 49.9%, respectively, along with DA-s-SP (0.1%) in the LS-SL indirect comparison. DA-LS was the most influential contributor to the entire network (23.5%), while DA-s-SP contributed 12.3% (**Fig. 8B**). Inconsistency was not found at either the global (p =0.92) or local level (DA-ISL p-value=0.92, DA-s-SP p-value=0.92, and ISL-s-SP p-value=0.92), which was confirmed when evaluating the network forest plot, where it was possible to graphically represent effect size by study (**Fig. 8C**). Indeed, the effect size by device is shown in the interval plot (**Fig. 8D**): s-SP overestimated in comparison with DA, while LS, ISL, and SP were closely comparable to DA, despite their large C.Is. and P.Is. could result in over-or underestimated measurements in future studies.
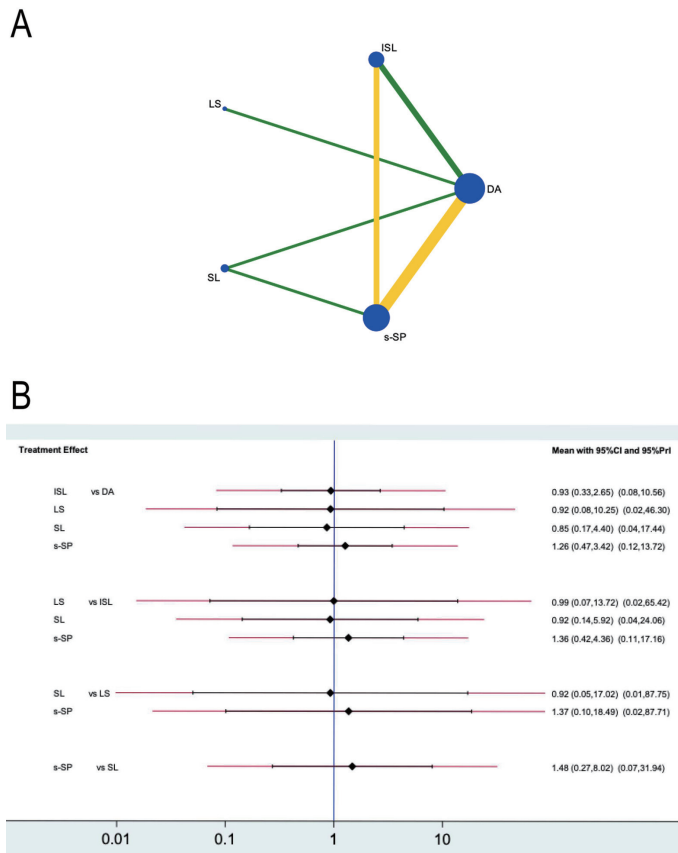
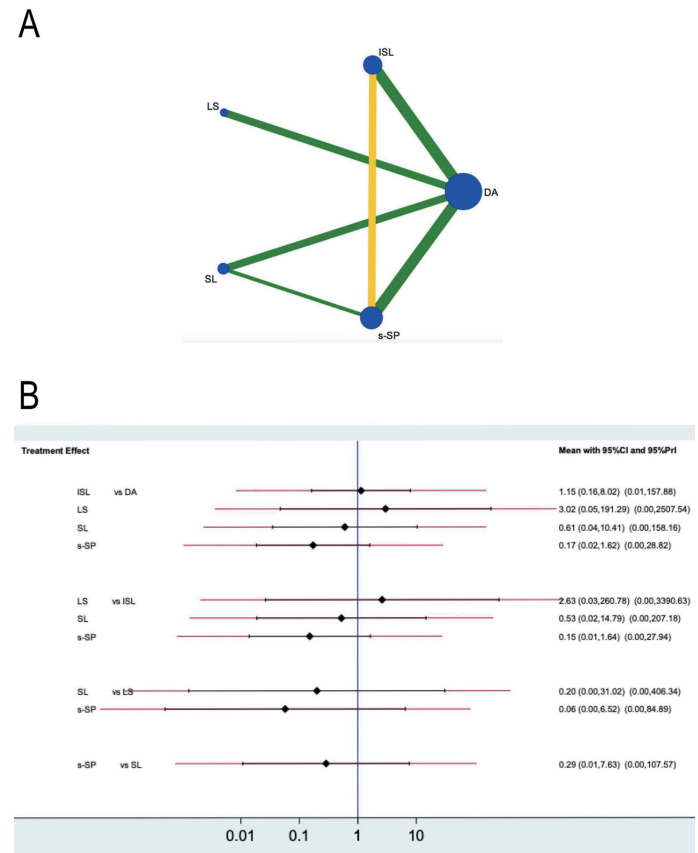**Fig. 3.** NMA for En-En measurement. A= Network Plot, B= Interval Plot.



**Fig. 4.** NMA for Ex-Ex measurement. A= Network Plot, B= Interval Plot.

## 4. DISCUSSION

Face-scans increase the degree of communication with the patient and enhance various aspects of the daily workflow[46]. It seems clear that the acquisition of extra-oral information can improve preparatory clinical evaluations, treatment plans, and follow-up documentation for various patients[47].

Ayaz et al. reported that 2D had a higher error rate than DA; however, comparing 2D with LS and p-SP showed no significant differences[40]. Indeed, there might be the possibility of introducing higher errors with respect to DA and 3D scans for the broader learning curve related to the problem of standardizing images, such as magnification, distortions, lighting, and object-camera distance[29].

Traditionally, digital smile design combines information obtained from two-dimensional photographs of the face and teeth[48].

The superimposition of the different surfaces of the various scans allows matching of the facial scans with intraoral scans and the three-dimensional radiodiagnostic investigations[49].

The result obtained from this rendering process allows us to obtain all the information regarding the face, teeth, soft tissues, and bone structures that can be integrated in a CAD-CAM process[50,51].

There is evidence in the literature regarding the accuracy of various techniques used for the acquisition of CBCT and intraoral impres-

sions[52].

Facial scans allow the orientation of the facial planes and integration into the workflow of the facebow fork concept to obtain mock-ups and easily integrated prostheses[53].

When working with facial scans, it is often necessary to superimpose several scans to evaluate the patient's face at rest, while smiling, and with extraoral landmarks anchored to the dental arches[54]. This is made possible by the different types of facial extraoral landmarks. An article by Pinto et al. showed that stereophotogrammetry provided good reproducibility in the superimposition of a face at rest and while smiling. This is not easily achievable using two-dimensional photography[55].

Notably, the mounting of the digital articulator can be done through cephalometric images using a facial scanner, digital axiography, or standardized extra-oral photos[56–59].

### 4.1 Overview of Technologies

To obtain a three-dimensional image of the face, regardless of the system used, sensors are required. The sensors are located inside scanners and cameras and are divided into active and passive sensors.

The active scanner emits signals that bounce off an object located in the immediate vicinity of the device. A passive scanner de-
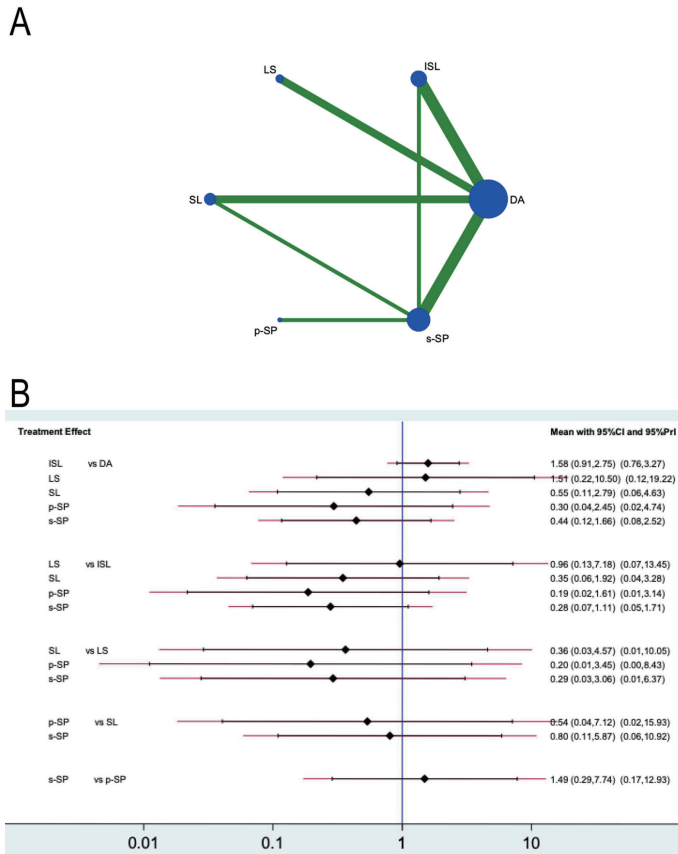
**Fig. 5.** NMA for Ch-Ch measurement. A= Network Plot, B= Interval Plot.



**Fig. 6.** NMA for Al-Al measurement. A= Network Plot, B= Interval Plot.

tects changes in infrared or visible light to an object from various distances to create an image.

Photogrammetry is one of the most accurate facial digitization options. It is characterized by a passive sensor and is divided into two techniques: stereophotogrammetry (static) and monoscopic photogrammetry (Portable).

In the first technique[9,19,23-26,28,31-35,38,41,43], all images are captured by different cameras simultaneously, and the cameras are placed at different angles and heights with respect to the subject. This guarantees reduced acquisition times, resolution, and precision comparable to direct anthropometry. These devices have many cameras that shoot simultaneously and may have integrated three-dimensional reconstruction software. They perform very well in terms of acquisition times for devices using this technology, which are very low and, on average, less than a second. However, they are expensive, require dedicated space, and cannot be easily disassembled[24]. It is also necessary to calibrate the device for each patient with a considerable waste of time[32,33].

A cheaper alternative to stereophotogrammetry is to use various individual photographic cameras arranged around the subject in a fixed configuration. This facial camera system requires a minimum of two cameras to scan the face but can also include more cameras[36]. Sailer et al.[36] demonstrated stereophotogrammetry acquisition with six reflex cameras connected to a PC and equipped with software for 3D reconstruction.
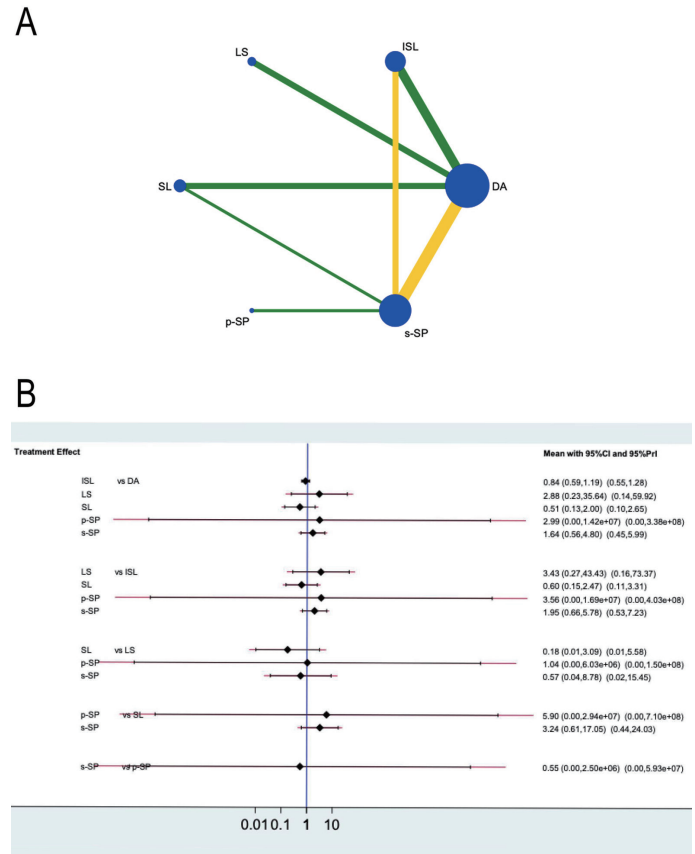
The monoscopic photogrammetry technique uses a single camera that captures different images at different angles and heights[32-34,39,41]. Gibelli et al. showed that portable systems have lower repeatability than stationary instruments and slower three-dimensional processing[33].

The Vectra H1/H2 (Canfield Scientific, Parsippany, NJ, USA) is a portable and compact device, the size of a normal type of camera, and uses monoscopic photogrammetry. Vectra H2 has a larger field of view than H1. Once the frames have been captured, they are uploaded to three-dimensional image processing software[28].

Laser scanners are based on trigonometric triangulation and utilize the detection of a reflected laser beam to reconstruct 3-D images[18,21,22,27,40]. This method is called triangulation because the laser point (or line), sensor, and laser emitter form a triangle. This scanner uses active sensors and is positioned at a known distance from the laser source; therefore, it is possible to make precise measurements of the points by calculating the angle of reflection of the laser light. Knowing the distance between the scanner and the object, the scanning hardware can map the surface of the object and record a 3D scan.

Critical parts for acquisition are the ears, nose wings, and chin; shadows and a dark complexion usually result in a hampered scan. The main limitations of laser scanners are the cost and size of the devices. In addition, scans should be performed with the eyes closed to avoid direct contact between the laser beam and the eyes[18,27].
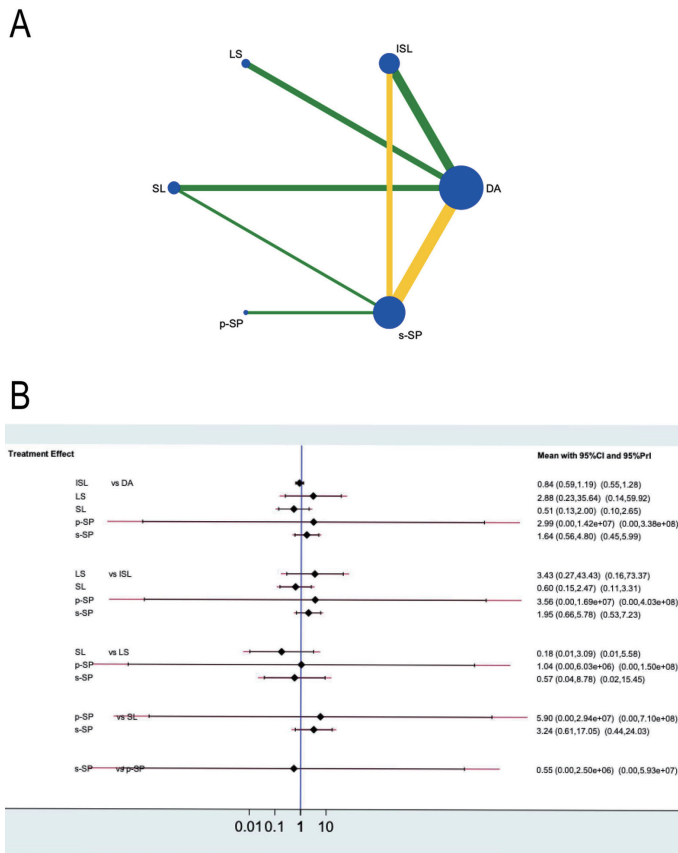
Fig. 7. NMA for N-Sn measurement. A= Network Plot, B= Interval Plot.



Fig. 8. NMA for T-Pg measurement. A= Network Plot, B= Interval Plot.

Modern CBCT equipment with this integrated function has reduced scanning time with improved results[40].

The Structured Light technology employs trigonometric triangulation but works by projecting a light pattern onto the face to be scanned[20,28,30,37,38]. This technology also employs active sensors. One or more sensors (or cameras) observe the shape of the light pattern and calculate the distance between each point in the field of view. The advantage of structured light technology is the speed of the scans, and it is not necessary to protect the patient's eyes or body from ionizing or laser radiation[30,38]. One of the disadvantages of this type of scanner is that it is sensitive to the lighting conditions in a given environment. Some studies have reported how the light of these devices using visible light sources disturbs the eyes of patients, and it is problematic for people with a history of seizures.

Infrared-structured light scanners use a hybrid light source, infrared light, and structured light. In recent years, research and potential applications have expanded, aimed at identifying methods of integration between different sensors, such as offering superior detection skills to standardized techniques. The invisible infrared light source provides a reliable solution to the problem of acquiring dark-colored objects and allows easy acquisition of human hair[9,12,35,38,39,42-45].

Badr et al. showed in their study five modular units of Kinect (Microsoft Scanner) used to generate a 3D model of the face and to avoid image loss 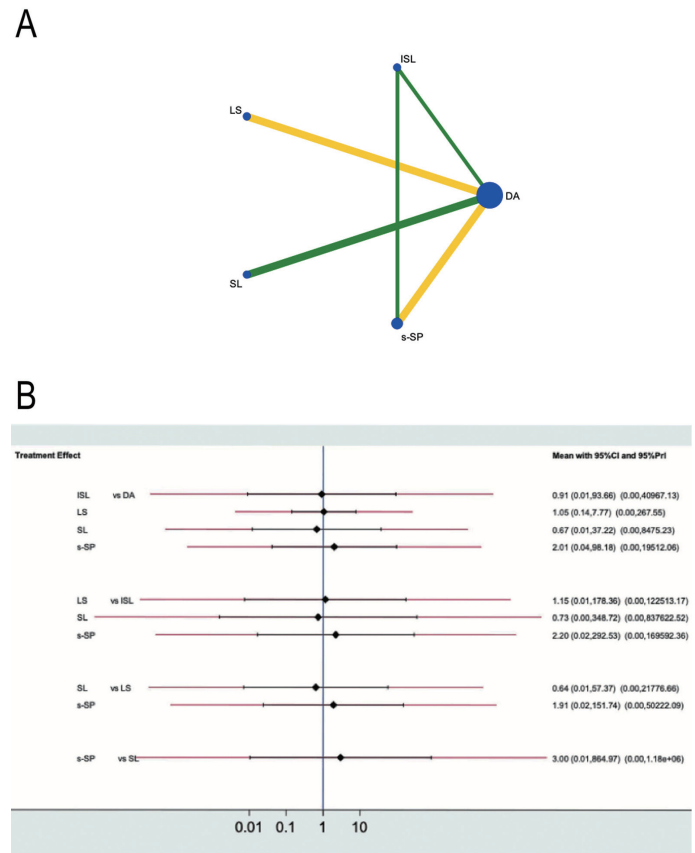on the whole face, including the ear region[44]. Thus, an economical and practical alternative provides excellent results.

The market has introduced tablets and smartphones capable of capturing surfaces through structured infrared light and processing them through apps that simulate photogrammetry.

Iphone 13 and Ipad Pro 3rd Gen. (Apple Store, Cupertino, CA, USA) use a technology that combines structured light with an infrared laser (TrueDept®) and photogrammetry based on application protocols. The camera system includes infrared, ambient light, and proximity sensors and dot projectors. To map facial anatomy, sensors and components work together to project 30 000 infrared dots onto the user's face. The facial scanning app FaceApp (Bellus3D inc) uses the device's internal camera and can perform a high-registration 3D face scan, in a single procedure by moving the subject's head or rotating the device itself, from left to right in approximately ten seconds. These applications sometimes contain voices that guide a patient's movement to increase the quality of the scans[42].

Finally, **Table 3** summarizes the guidelines needed to obtain the most accurate scanning, regardless of the type of technology.

### 4.2 Discussion of Findings

The issue of face scanners has become so relevant that, in recent years, several authors have reviewed the development of this technology in the medical field. In past revisions, the technologies identified were the same as those we evaluated, except for ISL, which

**Table 3.** Suggestion chart. This table makes explicit tips for obtaining high-quality scans extracted from the analyzed articles.

| Issue | Suggestion |
|---|---|
| *Illumination* | The illumination of the room and the scanned subject. Certainly, a specific lighting kit can enhance the quality of the image acquisition |
| *Position of patient and scanner* | The inclination of the subject should always be perpendicular to the floor, paying attention to any pro- or retro-tilt of the seat support that may alter the acquisition. Certainly, the patient should be instructed and informed of the procedures before scanning so that they are adequately prepared. Regarding the position of the scanning technology please refer to the manufacturer's instruction booklet. |
| *Micro-movements* | To the reduction of micro-movements: controlled rotation of the device and stationary subject has produced good results, but the gold standard remains scanning through multiple units or static stereophotogrammetry that allows simultaneous acquisition at different angles. The position of the subject should be comfortable and relaxed, different inclinations can lead to increased involuntary movements created by muscle tension and consequently worsen the quality of the scan. It is recommended to always check the scans before dismissing the patient. |
| *Facial landmarks* | the white sticker technique with a black dot in the middle seems to be the most accurate and able to reduce interoperator variability, also oral and frontal supports provided by some companies seem to be a faster and more effective choice. |

was introduced more recently. Pestrides et al.[13] reported a technology called "RGB-D sensors, " which are similar to infrared-structured light. Moreover, previous reviews have included both dummy and cadaver scans. This is to assess the validity of the scan and its repeatability. However, as these reviews have also concluded, the presence of artifacts due to a living subject is one of the most critical factors. This is the reason why this review focused only on live subjects and attempted to illustrate the characteristics of the various technologies used in clinical practice. Two previous reviews employed quantitative analysis by pairwise meta-analysis[6,10]. Although this type of analysis offers excellent possibilities for reviewing data from various studies, it requires predetermined and equal pairs and does not allow us to compare various technologies. In contrast, our type of NMA enabled us to include more studies and draw conclusions from both direct and indirect comparisons. However, the most relevant thing is that, in contrast to previous reviews that collected average values of the whole scan, we decided to split the linear measures into three subgroups according to the X, Y, and Z planes. This was achieved by grouping segments almost parallel to the investigated planes.

The horizontal segments (En-En, Ex-Ex, Al-Al, and Ch-Ch) are representative of areas in which microexpressions can create inaccuracies. They were also distributed over one-third of the face. On the other hand, the vertical segment representing the height of the nose is not very susceptible to microexpressions because it lacks muscles. The sagittal segment representing the depth of the jaw is very relevant as it is affected by the coupling of various photos, as in the case of stereophotogrammetry and single-source ISL technologies, in which the patient is asked to rotate his head, a practice that produces artifacts in the scan. Of course, this type of data collection did not allow us to analyze many linear measurements; otherwise, we would have fallen into high data fragmentation by including only a few studies per group. However, as reported in other studies, we assumed that six linear measurements were sufficient to validate a face scan[12,22,26]. The last review on this topic focused on the difference between portable and static instruments, highlighting no significant differences between the devices. Gibelli et al. reported that s-SP and SL are the closest technologies to direct anthropometry, whereas LS tends to overestimate linear distances[10].

From our current experience, we can conclude that in the horizontal measurements, both for the nature of the data and for the wide C.Is, there are no significant differences, but we can discuss the trends. In agreement with the previous reviews on horizontal measurements, s-SP, p-SP, and SL tended to underestimate linear distances and thus have similar results, while ISL and LS tended to

overestimate distances. This was not true for En-En distance, where the trends were reversed. Twelve out of 16 horizontal measurements had a mean difference from DA less than 0.6 mm, two measurements less than 1 mm, and three measurements less than 2 mm (**Table 4**, **Table 5**, **Table 6**, **Table 7**). The largest differences were reported in the p-SP and s-SP groups in the Ex-Ex and Ch-Ch distances, because of the large involvement of these areas in facial expression. For vertical distance, we have all effect sizes close to each other and similar to DA and with generally small C.Is., the results can be considered quite significant. In this case, ISL and SL tended to slightly underestimate the distance, whereas the other technologies overestimated it. However, it is important to note that the mean difference of ISL and s-SP from DA is less than 0.6 mm (**Table 8**). For the sagittal measurement there are very large confidence intervals. This could be because this measurement is reported by a small number of included studies. The largest mean difference was in the s-SP technology (0.7 mm (**Table 9**). What emerged is that new and more user-friendly technologies are achieving results that could be compared accurately to DA, and s-SP and LS are expensive and tested devices. Furthermore, by widening the field, we can see that active technologies can often achieve more accurate results than passive technologies. Passive technologies can achieve better graphic image resolution, and measurements of the distances between the considered points deviate slightly from the DA.

Certainly, the results obtained by ISL are quite affected by two extremely recent studies: one[44] employs a 5-unit Microsoft Kinect v2 to obtain an image instantaneously with active technology, and the other[42] uses highly implemented software that can obtain excellent results. Unfortunately, this application is not available in Europe; therefore, we were not able to personally check the accuracy of this application.

It has already been noted how facial scans with intraoral and extraoral matching tools can operate as digital facebow[60]. It was also seen that scanning technology had a huge influence on the repeatability of scans, with a mean variability of 0.2 mm for SL and 0.4 to 1.02 mm for ISL[61].

An interesting study evaluated the transfer accuracy from analog to virtual articulator using a laboratory scanner (indirect methods) and reported an average trueness of 0.55 mm and maximum deviation of 1.02 mm[62]. Pending future studies comparing indirect and direct methods with facial scanning, we could establish that a deviation in terms of trueness and repeatability of less than 0.60 mm can be considered acceptable for restorative procedures.

**Table 4.** Mean Difference Ex-Ex. This table report the mean difference between test and control groups of Ex-Ex distances in NMA included studies.

| Mean difference | Coef. | Std. Err. | Z score | P-value | [95% Conf. Interval] | |
|---|---|---|---|---|---|---|
| ISL – DA | 0.1376393 | 0.9918229 | 0.14 | 0.890 | -1.806298 | 2.081576 |
| LS – DA | 1.104779 | 2.116893 | 0.52 | 0.602 | -3.044256 | 5.253813 |
| SL – DA | -0.5005741 | 1.450774 | -0.35 | 0.730 | -3.344039 | 2.342891 |
| s-SP – DA | -1.749799 | 1.138716 | -1.54 | 0.124 | -3.981643 | .4820437 |

DA= direct anthropometry, s-SP= Static Stereophotogrammetry, SL= Structured light, LS=Laser Scanner, ISL=Infrared Structured Light.

**Table 5.** Mean Difference En-En. This table report the mean difference between test and control groups of En-En distances in NMA included studies.

| Mean difference | Coef. | Std. Err. | Z score | P-value | [95% Conf. Interval] | |
|---|---|---|---|---|---|---|
| ISL – DA | -0.0733913 | 0.5348637 | -0.14 | 0.891 | -1.121705 | 0.9749224 |
| LS – DA | -0.08 | 1.228111 | -0.07 | 0.948 | -2.487054 | 2.327054 |
| SL – DA | -0.1580372 | 0.8367269 | -0.19 | 0.850 | -1.797992 | 1.481917 |
| s-SP – DA | 0.2319346 | 0.5085988 | 0.46 | 0.6448 | -0.7649008 | 1.22877 |

DA= direct anthropometry, s-SP= Static Stereophotogrammetry, SL= Structured light, LS=Laser Scanner, ISL=Infrared Structured Light.

**Table 6.** Mean Difference Ch-Ch. This table report the mean difference between test and control groups of Ch-Ch distances in NMA included studies.

| Mean difference | Coef. | Std. Err. | Z score | P-value | [95% Conf. Interval] | |
|---|---|---|---|---|---|---|
| ISL – DA | 0.4581373 | 0.2826558 | 1.62 | 0.105 | -.0958579 | 1.012132 |
| LS – DA | 0.4123463 | 0.9894147 | 0.42 | 0.677 | -1.526871 | 2.351563 |
| SL – DA | -0.5999546 | 0.8299848 | -0.72 | 0.470 | -2.226695 | 1.026786 |
| p-SP – DA | -1.220762 | 1.080069 | -1.13 | 0.258 | -3.337658 | .8961335 |
| s-SP – DA | -0.8207623 | 0.6786372 | -1.21 | 0.226 | -2.150867 | .5093422 |

DA= direct anthropometry, s-SP= Static Stereophotogrammetry, SL= Structured light, LS=Laser Scanner, ISL=Infrared Structured Light.

**Table 7.** Mean Difference Al-Al. This table report the mean difference between test and control groups of Al-Al distances in NMA included studies.

| Mean difference | Coef. | Std. Err. | Z score | P-value | [95% Conf. Interval] | |
|---|---|---|---|---|---|---|
| ISL – DA | 0.7188664 | 0.3909873 | 1.84 | 0.066 | -0.0474546 | 1.485187 |
| LS – DA | -0.0306535 | 0.5110322 | -0.06 | 0.952 | -1.032258 | 0.9709512 |
| SL – DA | 0.5438333 | .6854764 | 0.79 | 0.428 | -.7996757 | 1.887342 |
| s-SP – DA | -0.4205465 | .7600442 | -0.55 | 0.580 | -1.910206 | 1.069113 |

DA= direct anthropometry, s-SP= Static Stereophotogrammetry, SL= Structured light, LS=Laser Scanner, ISL=Infrared Structured Light.

The QUADAS-2 tool is suitable for assessing the quality of studies investigating diagnostic accuracy. The present review reports a risk of bias tending towards the lower end, the main doubts being represented by the index test domain, where the blindness of the assessors is not always clearly expressed. In studies on living people, the applicability is at its maximum. As many studies have reported, the presence of a beard, moustache, and hair on the face may prevent the correct detection of cephalometric points such as the tragus, anterior nasal spine, or lower orbital margin. These points may prevent the identification of some useful planes for prosthetic planning. Although the matching could be done by an extraoral fork, identifying these points could be useful in the digital wax-up procedure[12]. It is also difficult to apply these technologies to non-cooperative patients who are unable to remain motionless and control their facial expressions[54].

Although the data reported minimal deviations of sagittal measurement from DA, many articles reported difficulties in acquiring this point accurately[19,20,29,34,37]. Further studies reporting standard sagittal measurements are needed to clarify this issue. One of the limitations of this study is that it does not consider the performance of technologies applied directly to digital workflows. In addition to the image acquisition procedures, subsequent matching operations can introduce errors. Furthermore, the placement of landmarks before or after scanning and the marking technique can influence the linear measurements.

Today, much work is being done to introduce the fourth dimension into digital flow, where the previous data will be joined by mandibular dynamics, digital axiography, and muscle tone[63]. A high-precision but accessible face scanner with a simple interface would certainly benefit clinicians practicing digital dentistry on a daily basis.

**Table 8.** Mean Difference N-Sn. This table report the mean difference between test and control groups of N-Sn distances in NMA included studies.

| Mean difference | Coef. | Std. Err. | Z score | P-value | [95% Conf. Interval] | |
|---|---|---|---|---|---|---|
| ISL – DA | -0.1737213 | 0.1773929 | -0.98 | 0.327 | -0.521405 | 0.1739624 |
| LS – DA | 1.057965 | 1.283496 | 0.82 | 0.410 | -1.45764 | 3.57357 |
| SL – DA | -0.6780945 | 0.6986881 | -0.97 | 0.332 | -2.047498 | 0.691309 |
| p-SP – DA | 1.096018 | 7.842169 | 0.14 | 0.889 | -14.27435 | 16.46639 |
| s-SP – DA | 0.4960189 | 0.547407 | 0.91 | 0.365 | -0.5768791 | 1.568917 |

DA= direct anthropometry, s-SP= Static Stereophotogrammetry, SL= Structured light, LS=Laser Scanner, ISL=Infrared Structured Light.

**Table 9.** Mean Difference T-Pg. This table report the mean difference between test and control groups of T-Pg distances in NMA included studies.

| Mean difference | Coef. | Std. Err. | Z score | P-value | [95% Conf. Interval] | |
|---|---|---|---|---|---|---|
| ISL – DA | -0.091816 | 2.363059 | -0.04 | 0.969 | -4.723327 | 4.539695 |
| LS – DA | 0.0471817 | 1.022032 | 0.05 | 0.963 | -1.955964 | 2.050327 |
| SL – DA | -0.4036219 | 2.051274 | -0.20 | 0.844 | -4.424045 | 3.616801 |
| s-SP – DA | 0.6965159 | 1.984887 | 0.35 | 0.726 | -3.19379 | 4.586822 |

DA= direct anthropometry, s-SP= Static Stereophotogrammetry, SL= Structured light, LS=Laser Scanner, ISL=Infrared Structured Light.

## 5. Conclusion

In conclusion, the main findings of the study seem to suggest that:

• Facial scans are a powerful method for capturing extraoral information and integrating it into digital flow.

• All types of face scanner technologies have achieved results comparable to anthropometry, with a difference often < 1 mm.

• Regardless of the scanner type, it is necessary to pay attention to the illumination, landmarks, micromovements, and position related to the patient (**Table 3**).

• An accuracy of less than 0.60 mm would allow face scan to be used as a digital facebow in everyday dentistry.

## Conflicts of interest

The authors declare that there are no conflict of interests.

## References

[1] Fradeani M. Esthetic Rehabilitation in Fixed Prosthodontics. 1st ed. Chicago: Quintessence; 2004.

[2] O'Grady KF, Antonyshyn OM. Facial asymmetry: three-dimensional analysis using laser surface scanning. Plast Reconstr Surg. 1999;104:928–37. https://doi.org/10.1097/00006534-199909040-00006, PMID:10654730

[3] Coachman C, Van Dooren E, Gürel G, Landsberg CJ, Calamita MA, Bichacho N. Smile design: From digital treatment planning to clinical reality. In: Cohen M, editor. Interdisciplinary Treatment Planning. Vol 2: Comprehensive Case Studies. Chicago: Quintessence; 2012. p. 119–74.

[4] Stanley M, Paz AG, Miguel I, Coachman C. Fully digital workflow, integrating dental scan, smile design and CAD-CAM: case report. BMC Oral Health. 2018;18:134. https://doi.org/10.1186/s12903-018-0597-0, PMID:30086753

[5] Lepidi L, Galli M, Grammatica A, Joda T, Wang HL, Li J. Indirect Digital Workflow for Virtual Cross-Mounting of Fixed Implant-Supported Prostheses to Create a 3D Virtual Patient. J Prosthodont. 2021;30:177–82. https://doi.org/10.1111/jopr.13247, PMID:32865872

[6] Mai HN, Kim J, Choi YH, Lee DH. Accuracy of Portable Face-Scanning Devices for Obtaining Three-Dimensional Face Models: A Systematic Review and Meta-Analysis. Int J Environ Res Public Health. 2020;18:94. https://doi.org/10.3390/ijerph18010094, PMID:33375533

[7] Lee SY, Kim H, Lee D, Park C. Superimposition of a cone beam computed tomography (CBCT) scan and a photograph: A dental technique. J Prosthet Dent. 2021;125:212–5. https://doi.org/10.1016/j.prosdent.2020.01.008, PMID:32165013

[8] Ritschl LM, Wolff KD, Erben P, Grill FD. Simultaneous, radiation-free registration of the dentoalveolar position and the face by combining 3D photography with a portable scanner and impression-taking. Head Face Med. 2019;15:28. https://doi.org/10.1186/s13005-019-0212-x, PMID:31767030

[9] Raffone C, Gianfreda F, Pompeo MG, Antonacci D, Bollero P, Canullo L. Chairside virtual patient protocol. Part 2: management of multiple face scans and alignment predictability. J Dent. 2022;122:104123. Epub ahead of print. https://doi.org/10.1016/j.jdent.2022.104123, PMID:35413410

[10] Joda T, Gallucci GO. The virtual patient in dental medicine. Clin Oral Implants Res. 2015;26:725–6. https://doi.org/10.1111/clr.12379, PMID:24665872

[11] Gibelli D, Dolci C, Cappella A, Sforza C. Reliability of optical devices for three-dimensional facial anatomy description: a systematic review and meta-analysis. Int J Oral Maxillofac Surg. 2020;49:1092–106. https://doi.org/10.1016/j.ijom.2019.10.019, PMID:31786104

[12] Piedra-Cascón W, Meyer MJ, Methani MM, Revilla-León M. Accuracy (trueness and precision) of a dual-structured light facial scanner and interexaminer reliability. J Prosthet Dent. 2020;124:567–74. https://doi.org/10.1016/j.prosdent.2019.10.010, PMID:31918895

[13] Petrides G, Clark JR, Low H, Lovell N, Eviston TJ. Three-dimensional scanners for soft-tissue facial assessment in clinical practice. J Plast Reconstr Aesthet Surg. 2021;74:605–14. https://doi.org/10.1016/j.bjps.2020.08.050, PMID:33082078

[14] Whiting PF, Rutjes AW, Westwood ME, Mallett S, Deeks JJ, Reitsma JB, et al.; QUADAS-2 Group. QUADAS-2: a revised tool for the quality assessment of diagnostic accuracy studies. Ann Intern Med. 2011;155:529–36. https://doi.org/10.7326/0003-4819-155-8-201110180-00009, PMID:22007046

[15] Hutton B, Salanti G, Caldwell DM, Chaimani A, Schmid CH, Cameron C, et al. The PRISMA extension statement for reporting of systematic reviews incorporating network meta-analyses of health care interventions: checklist and explanations. Ann Intern Med. 2015;162:777–84. https://doi.org/10.7326/M14-2385, PMID:26030634

[16] Puhan MA, Schünemann HJ, Murad MH, Li T, Brignardello-Petersen R, Singh JA, et al.; GRADE Working Group. A GRADE Working Group approach for rating the quality of treatment effect estimates from network meta-analysis. BMJ. 2014;349:g5630. https://doi.org/10.1136/bmj.g5630, PMID:25252733

[17] Chaimani A, Higgins JPT, Mavridis D, Spyridonos P, Salanti G. Graphical tools for network meta-analysis in STATA. PLoS One. 2013;8:e76654. https://doi.org/10.1371/journal.pone.0076654, PMID:24098547

[18] Joe PS, Ito Y, Shih AM, Oestenstad RK, Lungu CT. Comparison of a novel surface laser scanning anthropometric technique to traditional methods for facial parameter measurements. J Occup Environ Hyg. 2012;9:81–8. https://doi.org/10.1080/15459624.2011.640557, PMID:22214207

[19] Wong JY, Oh AK, Ohta E, Hunt AT, Rogers GF, Mulliken JB, et al. Validity and reliability of craniofacial anthropometric measurement of 3D digital photogrammetric images. Cleft Palate Craniofac J. 2008;45:232–9. https://doi.org/10.1597/06-175, PMID:18452351

[20] Weinberg SM, Scott NM, Neiswanger K, Brandon CA, Marazita ML. Digital three-dimensional photogrammetry: evaluation of anthropometric precision and accuracy using a Genex 3D camera system. Cleft Palate Craniofac J. 2004;41:507–18. https://doi.org/10.1597/03-066.1, PMID:15352857

[21] Kovacs L, Zimmermann A, Brockmann G, Gühring M, Baurecht H, Papadopulos NA, et al. Three-dimensional recording of the human face with a 3D laser scanner. J Plast Reconstr Aesthet Surg. 2006;59:1193–202. https://doi.org/10.1016/j.bjps.2005.10.025, PMID:17046629

[22] Ramieri GA, Spada MC, Nasi A, Tavolaccini A, Vezzetti E, Tornincasa S, et al. Reconstruction of facial morphology from laser scanned data. Part I: reliability of the technique. Dentomaxillofac Radiol. 2006;35:158–64. https://doi.org/10.1259/dmfr/43516583, PMID:16618848

[23] Ghoddousi H, Edler R, Haers P, Wertheim D, Greenhill D. Comparison of three methods of facial measurement. Int J Oral Maxillofac Surg. 2007;36:250–8. https://doi.org/10.1016/j.ijom.2006.10.001, PMID:17113754

[24] Heike CL, Cunningham ML, Hing AV, Stuhaug E, Starr JR. Picture perfect? Reliability of craniofacial anthropometry using three-dimensional digital stereophotogrammetry. Plast Reconstr Surg. 2009;124:1261–72. https://doi.org/10.1097/PRS.0b013e3181b454bd, PMID:19935311

[25] Asi SM, Nur HI. Zainal AA R. "Validity and reliability evaluation of data acquisition using Vectra 3D compare to direct method." 2012 IEEE-EMBS Conference on Biomedical Engineering and Sciences. IEEE, 2012.

[26] Park JH, Sharma AA, Tai K, Iida S, Yanagi Y, Asaumi J, et al.. Correlation between direct anthropometry and Di3D camera system. J Hard Tissue Biol. 2012;21:87–92. https://doi.org/10.2485/jhtb.21.87

[27] Lippold C, Liu X, Wangdo K, Drerup B, Schreiber K, Kirschneck C, et al. Facial landmark localization by curvature maps and profile analysis. Head Face Med. 2014;10:54. https://doi.org/10.1186/1746-160X-10-54, PMID:25488063

[28] Ye H, Lv L, Liu Y, Liu Y, Zhou Y. Evaluation of the Accuracy, Reliability, and Reproducibility of Two Different 3D Face-Scanning Systems. Int J Prosthodont. 2016;29:213–8. https://doi.org/10.11607/ijp.4397, PMID:27148978

[29] Dindaroğlu F, Kutlu P, Duran GS, Görgülü S, Aslan E. Accuracy and reliability of 3D stereophotogrammetry: A comparison to direct anthropometry and 2D photogrammetry. Angle Orthod. 2016;86:487–94. https://doi.org/10.2319/041415-244.1, PMID:26267357

[30] Modabber A, Peters F, Kniha K, Goloborodko E, Ghassemi A, Lethaus B, et al. Evaluation of the accuracy of a mobile and a stationary system for three-dimensional facial scanning. J Craniomaxillofac Surg. 2016;44:1719–24. https://doi.org/10.1016/j.jcms.2016.08.008, PMID:27614543

[31] Naini FB, Akram S, Kepinska J, Garagiola U, McDonald F, Wertheim D. Validation of a new three-dimensional imaging system using comparative craniofacial anthropometry. Maxillofac Plast Reconstr Surg. 2017;39:23. https://doi.org/10.1186/s40902-017-0123-3, PMID:28894726

[32] Kim AJ, Gu D, Chandiramani R, Linjawi I, Deutsch ICK, Allareddy V, et al. Accuracy and reliability of digital craniofacial measurements using a small-format, handheld 3D camera. Orthod Craniofac Res. 2018;21:132–9. https://doi.org/10.1111/ocr.12228, PMID:29863289

[33] Gibelli D, Pucciarelli V, Cappella A, Dolci C, Sforza C. Are Portable Stereophotogrammetric Devices Reliable in Facial Imaging? A Validation Study of VECTRA H1 Device. J Oral Maxillofac Surg. 2018;76:1772–84. https://doi.org/10.1016/j.joms.2018.01.021, PMID:29458028

[34] Camison L, Bykowski M, Lee WW, Carlson JC, Roosenboom J, Goldstein JA, et al. Validation of the Vectra H1 portable three-dimensional photogrammetry system for facial imaging. Int J Oral Maxillofac Surg. 2018;47:403–10. https://doi.org/10.1016/j.ijom.2017.08.008, PMID:28919165

[35] Maués CPR, Casagrande MVS, Almeida RCC, Almeida MAO, Carvalho FAR. Three-dimensional surface models of the facial soft tissues acquired with a low-cost scanner. Int J Oral Maxillofac Surg. 2018;47:1219–25. https://doi.org/10.1016/j.ijom.2018.03.028, PMID:29705405

[36] Liu S, Srinivasan M, Mörzinger R, Lancelle M, Beeler T, Gross M, et al. Reliability of a three-dimensional facial camera for dental and medical applications: A pilot study. J Prosthet Dent. 2019;122:282–7. https://doi.org/10.1016/j.prosdent.2018.10.016, PMID:30948294

[37] Franco de Sá Gomes C, Libdy MR, Normando D. Scan time, reliability and accuracy of craniofacial measurements using a 3D light scanner. J Oral Biol Craniofac Res. 2019;9:331–5. https://doi.org/10.1016/j.jobcr.2019.07.001, PMID:31388482

[38] Koban KC, Perko P, Etzel L, Li Z, Schenck TL, Giunta RE. Validation of two handheld devices against a non-portable three-dimensional surface scanner and assessment of potential use for intraoperative facial imaging. J Plast Reconstr Aesthet Surg. 2020;73:141–8. https://doi.org/10.1016/j.bjps.2019.07.008, PMID:31519501

[39] Rudy HL, Wake N, Yee J, Garfein ES, Tepper OM. Three-Dimensional Facial Scanning at the Fingertips of Patients and Surgeons: Accuracy and Precision Testing of iPhone X Three-Dimensional Scanner. Plast Reconstr Surg. 2020;146:1407–17. https://doi.org/10.1097/PRS.0000000000007387, PMID:33234980

[40] Ayaz I, Shaheen E, Aly M, Shujaat S, Gallo G, Coucke W, et al. Accuracy and reliability of 2-dimensional photography versus 3-dimensional soft tissue imaging. Imaging Sci Dent. 2020;50:15–22. https://doi.org/10.5624/isd.2020.50.1.15, PMID:32206616

[41] White JD, Ortega-Castrillon A, Virgo C, Indencleef K, Hoskens H, Shriver MD, et al. Sources of variation in the 3dMDface and Vectra H1 3D facial imaging systems. Sci Rep. 2020;10:4443. https://doi.org/10.1038/s41598-020-61333-3, PMID:32157192

[42] Chong Y, Liu X, Shi M, Huang J, Yu N, Long X. Three-dimensional facial scanner in the hands of patients: validation of a novel application on iPad/iPhone for three-dimensional imaging. Ann Transl Med. 2021;9:1115. https://doi.org/10.21037/atm-21-1620, PMID:34430556

[43] Akan B, Akan E, Şahan AO, Kalak M. Evaluation of 3D Face-Scan images obtained by stereophotogrammetry and smartphone camera. Int Orthod. 2021;19:669–78. https://doi.org/10.1016/j.ortho.2021.08.007, PMID:34544662

[44] Badr AM, Refai WMM, El-Shal MG, Abdelhameed AN. Accuracy and Reliability of Kinect Motion Sensing Input Device's 3D Models: A Comparison to Direct Anthropometry and 2D Photogrammetry. Open Access Maced J Med Sci. 2021;9:54–60. https://doi.org/10.3889/oamjms.2021.6006

[45] Raffone C, Gianfreda F, Bollero P, Pompeo MG, Miele G, Canullo L. Chairside virtual patient protocol. Part 1: free vs Guided face scan protocol. J Dent. 2022;116:103881. https://doi.org/10.1016/j.jdent.2021.103881, PMID:34762986

[46] Hassan B, Giménez Gonzáles B, Tahmaseb A, Jacobs R, Bornstein MM. Three-dimensional facial scanning technology: applications and future trends. Forum Implantol. 2014;10:77–86.

[47] Hassan B, Gimenez Gonzalez B, Tahmaseb A, Greven M, Wismeijer D. A digital approach integrating facial scanning in a CAD-CAM workflow for complete-mouth implant-supported rehabilitation of patients with edentulism: A pilot clinical study. J Prosthet Dent. 2017;117:486–92. https://doi.org/10.1016/j.prosdent.2016.07.033, PMID:27881321

[48] Coachman C, Calamita M, Sesma N. Dynamic Documentation of the Smile and the 2D/3D Digital Smile Design Process. Int J Periodontics Restorative Dent. 2017;37:183–93. https://doi.org/10.11607/prd.2911, PMID:28196157

[49] Mangano C, Luongo F, Migliario M, Mortellaro C, Mangano FG. Combining Intraoral Scans, Cone Beam Computed Tomography and Face Scans: The Virtual Patient. J Craniofac Surg. 2018;29:2241–6. https://doi.org/10.1097/SCS.0000000000004485, PMID:29698362

[50] Joda T, Brägger U, Gallucci G. Systematic literature review of digital three-dimensional superimposition techniques to create virtual dental patients. Int J Oral Maxillofac Implants. 2015;30:330–7. https://doi.org/10.11607/jomi.3852, PMID:25830393

[51] Coachman C, Calamita MA, Coachman FG, Coachman RG, Sesma N. Facially generated and cephalometric guided 3D digital design for complete mouth implant rehabilitation: A clinical report. J Prosthet Dent. 2017;117:577–86. https://doi.org/10.1016/j.prosdent.2016.09.005, PMID:27836143

[52] Zarone F, Ruggiero G, Ferrari M, Mangano F, Joda T, Sorrentino R. Accuracy of a chairside intraoral scanner compared with a laboratory scanner for the completely edentulous maxilla: an in vitro 3-dimensional comparative analysis. J Prosthet Dent. 2020;124:761.e1–7. https://doi.org/10.1016/j.prosdent.2020.07.018, PMID:33289647

[53] Li J, Chen Z, Decker AM, Wang HL, Joda T, Mendonca G, *et al.* Trueness and Precision of Economical Smartphone-Based Virtual Facebow Records. J Prosthodont. 2022;31:22–9. https://doi.org/10.1111/jopr.13366, PMID:33876857

[54] Gibelli D, De Angelis D, Poppa P, Sforza C, Cattaneo C. An assessment of how facial mimicry can change facial morphology: implications for identification. J Forensic Sci. 2017;62:405–10. https://doi.org/10.1111/1556-4029.13295, PMID:27907238

[55] Pinto PHV, Rodrigues CHP, Rozatto JR, Silva AMBR, Bruni AT, Silva MAMR, *et al.* Can a spontaneous smile invalidate facial identification by photo-anthropometry? Imaging Sci Dent. 2021;51:279–90. https://doi.org/10.5624/isd.20210002, PMID:34621655

[56] Joda T, Zarone F, Ferrari M. The complete digital workflow in fixed prosthodontics: a systematic review. BMC Oral Health. 2017;17:124. https://doi.org/10.1186/s12903-017-0415-0, PMID:28927393

[57] Solaberrieta E, Minguez R, Etxaniz O, Barrenetxea L. Improving the digital workflow: direct transfer from patient to virtual articulator. Int J Comput Dent. 2013;16:285–92. PMID:24555405

[58] Solaberrieta E, Otegi JR, Mínguez R, Etxaniz O. Improved digital transfer of the maxillary cast to a virtual articulator. J Prosthet Dent. 2014;112:921–4. https://doi.org/10.1016/j.prosdent.2014.03.021, PMID:24836282

[59] Solaberrieta E, Garmendia A, Minguez R, Brizuela A, Pradies G. Virtual facebow technique. J Prosthet Dent. 2015;114:751–5. https://doi.org/10.1016/j.prosdent.2015.06.012, PMID:26372628

[60] Lepidi L, Galli M, Mastrangelo F, Venezia P, Joda T, Wang HL, *et al.* Virtual Articulators and Virtual Mounting Procedures: Where Do We Stand? J Prosthodont. 2021;30:24–35. https://doi.org/10.1111/jopr.13240, PMID:32827222

[61] Amezua X, Iturrate M, Garikano X, Solaberrieta E. Analysis of the impact of the facial scanning method on the precision of a virtual facebow record technique: An in vivo study. J Prosthet Dent. 2021 Dec 13:S0022-3913(21)00624-7.

[62] Úry E, Fornai C, Weber GW. Accuracy of transferring analog dental casts to a virtual articulator. J Prosthet Dent. 2020;123:305–13. https://doi.org/10.1016/j.prosdent.2018.12.019, PMID:31227241

[63] Jreige CS, Kimura RN, Segundo ÂRTC, Coachman C, Sesma N. Esthetic treatment planning with digital animation of the smile dynamics: A technique to create a 4-dimensional virtual patient. J Prosthet Dent. 2021 Feb 9:S0022-3913(20)30600-4. doi: https://doi.org/10.1016/j.prosdent.2020.10.015.